

Experimental Analysis and Modeling of a Stormwater Perlite Filter

Jorge Gironás^{1*}, José M. Adriasola², Bonifacio Fernández²

ABSTRACT: This paper presents the study of a mixed porous media composed of expanded perlite and a nonwoven needle-punched geotextile used to reduce the suspended solids load and concentration in urban runoff. Laboratory procedures were designed to quantify the suspended solids removal efficiency and variation in time of filtration rate. Different grain-size distributions of expanded perlite, diverse suspended solids concentrations, and different hydraulic and geometric conditions were tested to determine the most effective filter media. A dimensionless parameter, termed *Global Performance Index* (GPI), was developed to reach this objective. Measured data were also used to build a dimensional and a regression model to represent the performance of the filter media mathematically. The theory, derivation, and performance of both models are presented and compared with an existent empirical model. The dimensional model better reproduces the observations, becoming a useful tool for the design, operation, and evaluation of commercial porous media filters. *Water Environ. Res.*, **80**, 524 (2008).

KEYWORDS: expanded perlite, stormwater filter, suspended solids, stormwater runoff, water quality, best management practices.

doi:10.2175/193864708X267432

Introduction

Stormwater infiltration is a common technique used in best management practices for urban stormwater drainage and control. This technique reduces runoff discharges and volumes and promotes groundwater recharge. However, there are also some negative effects associated with infiltration, such as the risk of groundwater contamination and the reduction of the infiltration rate through time, as a result of infiltration surface clogging (Dechesne et al., 2002; Raimbault et al., 2000; Urbonas, 1999). One of the alternatives to control these problems is to use stormwater filters, which reduce the suspended solids load and concentration before stormwater reaches the infiltration areas (Urbonas, 1999; Urbonas and Stahre, 1993).

It is expected that any solution should be easy to implement, operate, and maintain. In the specific case of a modular stormwater filter device, it must be easy to install, clean, and renew; its size must be reduced; and it has to be built based on standardized elements, which facilitate the achievement of different design criteria by minimum changes or additions. To accomplish these objectives, the filter media must be carefully selected.

This article presents a preliminary investigation of expanded perlite as an alternative porous media to be used in stormwater filter

devices, which help to reduce suspended solids loads and concentrations in urban stormwater. The paper is organized as follows. The first section describes the filter media used in this study, the main characteristics of the filter media, and the reasons supporting this selection. The next section presents the experimental measurements, depiction of the main variables that characterize the performance of the filter media, analysis of the experiments results, and a comparison of different design alternatives. These results are used to develop different models, which are discussed and compared in the next section. Concluding remarks are offered in the final section of the paper.

Filter Media Selection

Several materials have been reported as filter media in the literature. Clark and Pitt (1999) summarize the most current and widely used media, including sand, activated carbon, and peat moss. Each has advantages and limitations, and the selection depends on the desired pollutant removal performance and associated conditions, such as land use (Clark and Pitt, 1999). Most of these filters must be built in situ because of the amount of material needed to reach good performance and because of the large concrete structures involved in the construction.

An alternative approach can be the design of small, easy-to-install filter devices that do not require a complicated building process and are used to treat smaller draining areas. Additionally, a filter device should be designed to achieve high filtration rates and removal efficiency. From that point-of-view, it is very important to select a filter media that meets the following properties: (1) high specific surface area; (2) low mass density, allowing an easy installation and transportation of the filter and/or the filter media; and (3) structural resistance to handle typical installation and operation loads.

A material that satisfies these characteristics is expanded perlite. Perlite is a natural siliceous rock that, when heated to a suitable point in its softening range (760 to 1100°C), expands 4 to 20 times its original volume, reaching an extremely light weight and a high specific surface area (Purchas, 1997). This expansion is the result of the presence of a significant percentage of combined water in the crude rock. Figure 1 presents the different states for the perlite, while Figure 2 shows the very complex porous microstructure of expanded perlite. Some of its typical applications are in the construction, agriculture, food, beverage, medical, and chemical industries (Uluatam, 1991). Expanded perlite has already been used and studied as a filter media to treat residential and industrial wastewater (Demirbas et al., 2002; Dogan and Alkan, 2003; Dogan et al., 2004; Joseph and Rodier, 1994; Uluatam, 1991). Additionally, perlite and expanded perlite have also been used as stormwater filter media or as a component with other materials (Adriasola, 2003; CALTRANS, 2004; CONTECH Stormwater Solutions Inc., 2002a, 2002b; Milesi

¹ Department of Civil and Environmental Engineering, Colorado State University, Fort Collins, Colorado.

² Departamento de Ingeniería Hidráulica y Ambiental, Pontificia Universidad Católica de Chile, Santiago, Chile.

* Department of Civil and Environmental Engineering, Colorado State University, Fort Collins Co. 80523, USA; e-mail: jorge.gironas@colostate.edu.



Figure 1—Natural and expanded perlite (Perlite Institute Inc., <http://www.perlite.org>).

et al., 2006; U.S. EPA, 2005; Wigginton and de Ridder, 1999). However, more research is required in testing and modeling the performance of this material, particularly the expanded perlite. Table 1 presents some physical properties of this mineral, according to the Perlite Institute Inc. (Harrisburg, Pennsylvania). Purchas (1997) provided a typical chemical composition of expanded perlite shown in Table 2. It can be seen that this material has the previously discussed properties of high specific surface area and low mass density. In particular, its specific surface area (S) is approximately 8 times larger than the specific surface area of sand, another typical filter media (Timmons et al., 2006). As a reference, typical values of S for other common filter media are as follows: 11.74 to 332.42 m^2/g for zeolite (Hernández et al., 2005); 1.2 to 1.6 m^2/g (Kleineidam et al., 2002; Zilli et al., 1996) or $270 \times 10^3 \text{ m}^2/\text{m}^3$ (Kennens and Thalasso, 1998; Ramírez-López et al., 2003) for peat; and $380 \times 10^3 \text{ m}^2/\text{m}^3$ for compost (Kennens and Thalasso, 1998; Smet et al., 1996).

For the final design of a standardized filter, it might be important to consider reductions in the thickness of the filtration layer. Additional filter media, such as nonwoven needle-punched geotextiles, which allow for the removal of fine particles not retained by the expanded perlite layer, can be used for this purpose. In addition, this type of geotextile controls the separation of fine particles from the filter media and facilitates a three-dimensional flux, which retards clogging.

Experimental Measurements and Results Analysis

A complete experimental methodology was developed to study the behavior of a mixed filter media composed of a main layer of expanded perlite and a nonwoven needle-punched geotextile located downstream, to remove fine particles not retained by the expanded perlite. This experimental study was carried out to evaluate the performance of the filter media under controlled conditions and gain experience in the potential application of expanded perlite as an

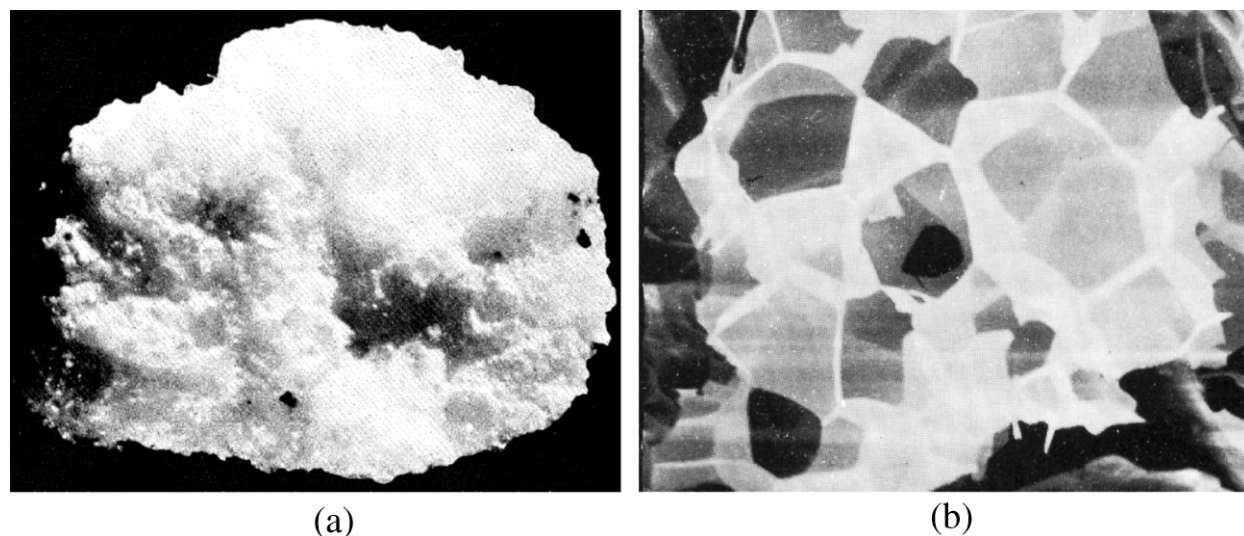


Figure 2—Structure of the expanded perlite: (a) grain of expanded perlite (Perlite Institute Inc., 2007) and (b) expanded perlite at high magnification (Dicalite, Gent, Belgium, <http://www.dicalite-europe.com>).

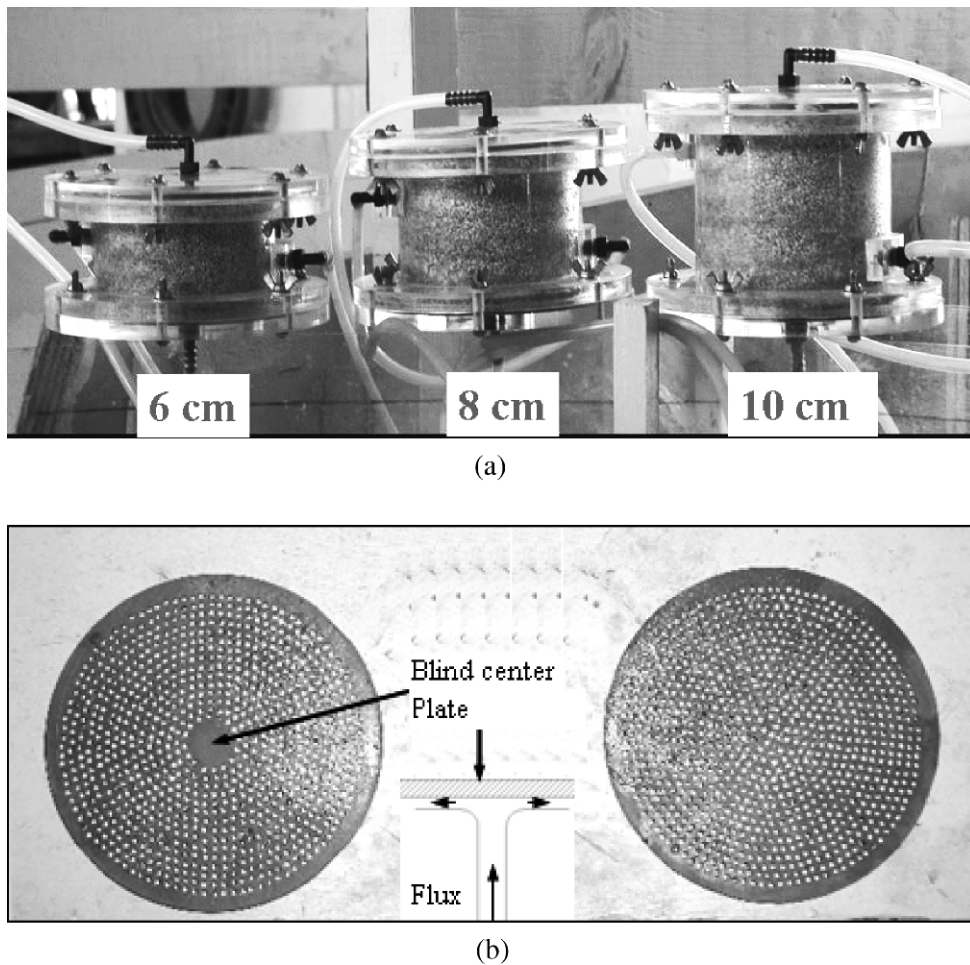


Figure 3—Experimental setup: (a) acrylic cells with different filter media thickness, (b) diffuser plates, (c) schematic representation, and (d) laboratory setup.

alternative filter media. Therefore, it cannot be assumed that the results presented here will completely explain the performance of the filter under long-term field conditions. The laboratory procedures were designed to quantify the most important variables that characterize the performance of the filter media—suspended solids efficiency removal (R) and variation in time of filtration rate (Q). Different grain-size distributions of expanded perlite, diverse

suspended solids concentrations, and different hydraulic and geometric conditions were tested to represent the typical conditions at which a stormwater filter would operate.

An additional objective was to determine which filter media was the most effective, in terms of removal capacity and maximization of the filtration rate.

Experimental Setup. A constant-head permeameter was used to supply mixtures of water and suspended solids at different

Table 1—Physical properties of expanded perlite.

Property	Value
Color	White
Maximum moisture	0.5%
pH	6.5 to 8.0
Specific gravity	2.2 to 2.4
Bulk density (loose weight, expanded form)	32 to 400 kg/m ³
Fusion point	1260 to 1343°C
Saturation porosity (for $d = 0.5$ to 1 mm)	84.93%
Specific surface area (for $d = 0.5$ to 1 mm)	0.72 m ² /g or 80.64 × 10 ³ m ² /m ³

Table 2—Chemical composition of expanded perlite.

Component	Percent weight
SiO ₂	74.70
Al ₂ O ₃	13.20
K ₂ O	5.08
Na ₂ O	4.40
CaO	0.83
Fe ₂ O ₃	0.67
MgO	0.03
TiO ₂	0.01
P ₂ O ₅	<0.01
Others	1.00

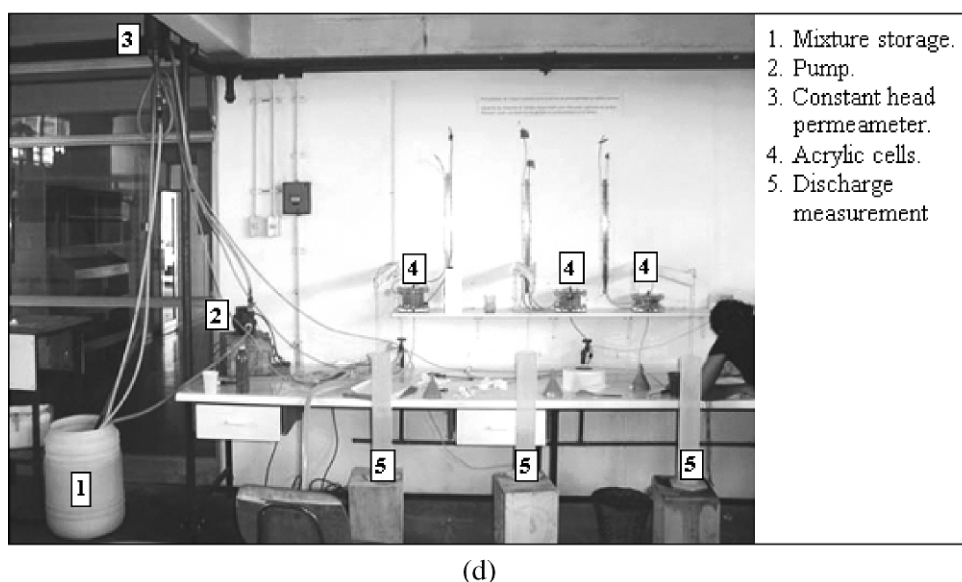
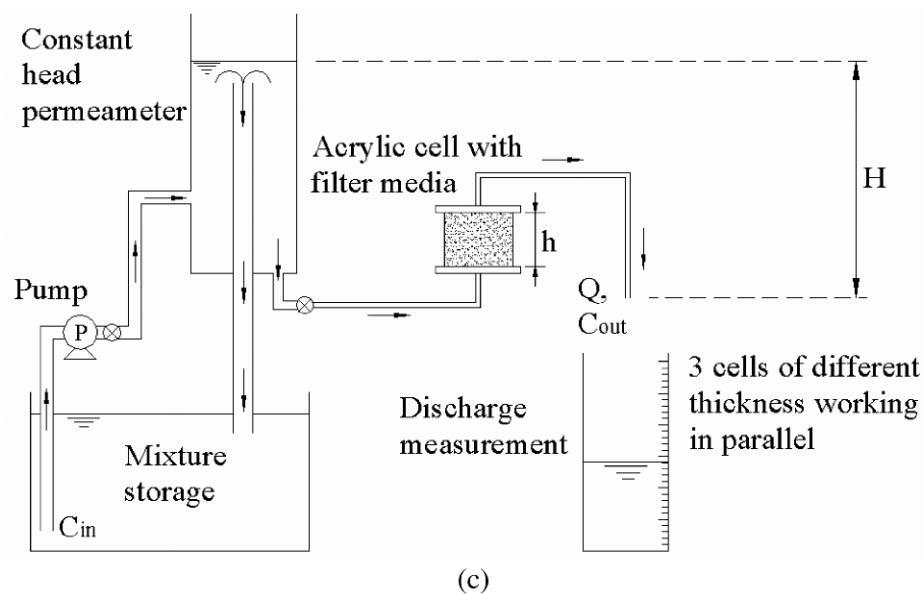


Figure 3—(Continued)

concentrations through diffuser plates to three cylindrical acrylic cells 10 cm in diameter. The cells had filter media samples of 6, 8, and 10 cm of thickness (h). The experiments were run using a constant head, to reduce possible factors affecting the performance of the filter and clearly understand the behavior of the filter media itself. However, stormwater filters in real conditions rarely operate under a constant head, so further studies with a variable head are necessary to better understand the performance of the filter media in field conditions. Figure 3 shows the experimental setup.

Filter Media. Three different types of expanded perlite were used—A-4, A-6, and A-5, with A-5 being a combination of 50% of the first two classes. Figure 4 presents the particle-size distributions for each type of expanded perlite, while Table 3 shows their main characteristics. The main characteristics of the nonwoven needle-punched geotextile used are presented in Table 4.

Concentration and Particle-Size Distribution of Suspended Solids. Typical silica from a fluvial source was used as the

suspended solids in the experiments. Influent concentrations of suspended solids used in the experiments were comparable with those observed in stormwater runoff in Chile, which varied from 50 mg/L in small and controlled urban catchments to 2000 mg/L in large catchments (MOP- DICTUC, 2001). The idea was to intentionally evaluate the performance of the filter media under the concentrations reported by this study; therefore, no target removal efficiency was used as a goal. Because of difficulties in keeping a constant input concentration, mainly as a result of the solids addition and mixture processes, it was decided to work with ranges rather than constant concentrations. These ranges were measured and controlled in each experiment. The particle-size distribution of suspended solids used in the water samples is similar to those commonly observed in stormwater runoff and presented by the Rinker Material Corporation (2002). The methodology used to determine this distribution was based on the American Society for Testing and Materials (West Conshohocken, Pennsylvania)

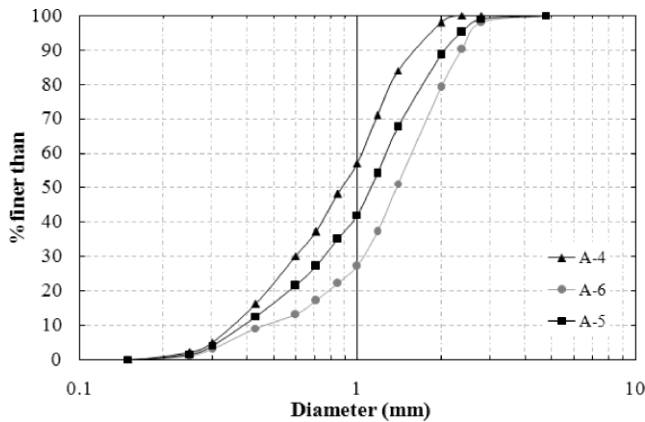


Figure 4—Particle-size distribution of the three types of expanded perlite.

(ASTM) procedure C136-96a (ASTM, 1997). Turbidity measures, obtained with a turbidimeter (Orbeco Hellige 965-10, Farmingdale, New York), were used to estimate the concentration of suspended solids using a fitted curve relating turbidity and concentration, as presented in Figure 5. Suspended solids concentrations were calculated using *Standard Method 2540D* (APHA et al., 1998). Figure 6 presents the particle-size distribution of suspended solids.

Methodology and Results. Forty-six filtration processes were simulated for different concentrations (50 to 1200 mg/L), constant heads (35 and 80 cm), durations (4.55 to 33 hours), types of expanded perlite (A-4, A-6, and A-5), and layer thickness (6, 8, and 10 cm). The variables measured in each experiment were the input turbidity (every 30 minutes); output turbidity (every 5 minutes); and discharges, which were measured using a volume of 2 L. With this information, the filtration rates (Q) were computed with the input and output concentrations (C_{inp} and C_{out}), which were calculated using the relationship in Figure 5. Additionally, other important variables were calculated, such as the input and removed mass and the removal efficiency (R). After finishing each experiment, the expanded perlite layer and geotextile were completely replaced and the acrylic cell was totally washed and dried to commence with a new experiment.

A dimensionless parameter, termed *Global Performance Index* (GPI), was developed to compare different experiments, as follows:

$$GPI(t = T) = \frac{\forall}{H} \cdot R_T \quad (1)$$

Where

\forall = cumulative specific filtered volume at a particular time, T (m^3/m^2);

H = hydraulic head (m); and

R_T = total efficiency removal at time, T , which corresponds to the ratio between the total cumulative removed mass and the total mass of suspended solids entering to the filter.

$$R_T = \frac{\int_0^T (C_{inp} - C_{out}) \cdot Q \cdot dt}{\int_0^T C_{inp} \cdot Q \cdot dt} \quad (2)$$

Where

C_{inp} = input concentration (g/m^3),
 C_{out} = output concentration (g/m^3), and
 Q = discharge or filtration rate (m^3/s).

The GPI couples quality and quantity characteristics and is used to determine the most effective filter media, in terms of removal capacity and maximization of the filtration rate, permitting the selection of the thickness and type of expanded perlite for the filter. The main assumption in developing this index is that the filtration rate is linearly proportional to the head, H . This linear proportionality, proposed according to Darcy’s Law, can be easily noticed when clear water is passing through the porous media. Although this relation is not strictly valid when dirty water is being used, it can be assumed that the linearity remains, and, at the same time, the qualitative aspects that disturb the linearity can be isolated and considered as part of the variable R_T . From eq 1, it is seen that H is in the denominator, implying that the filtered volumes \forall are somehow standardized, allowing the simultaneous evaluation of experiments developed under different hydraulic heads. One drawback of the formulation here proposed to evaluate the performance of the filter media is the assumption of precise measurement of the variables involved in the GPI. Particularly, there may be a significant uncertainty in the quantification of R_T , which can affect the selection of the best filter media using this parameter. If no precise measurements of removed mass are available, it is suggested to use a discrete number representing a range of R_T , rather than the measured value of this variable.

The GPI was calculated for $T = 1, 2, 3, 4, 5$, and 6 hours. Based on the results of the experiments, an exponential fitting was used to determine the filtration rate per unit of area, q , in cases where the duration of the experiment did not allow computation of the GPI for all the proposed times.

$$q = \frac{Q}{A} = a \cdot e^{-b \cdot t} \quad (3)$$

Where

A = cross-sectional area of the filter (m^2), and

a and b = parameters to be calibrated.

Obviously $a = q_{ini}$, the specific discharge at $t = 0$. Then, the cumulative specific filtered volume to be used in eq 1, when no measurement of \forall is available, is given by the following:

$$\forall = \int_0^T q \cdot dt = q_{ini} \cdot \int_0^T e^{-b \cdot t} \cdot dt = \frac{q_{ini}}{b} \cdot (1 - e^{-b \cdot T}) \quad (4)$$

Where

q = filtration rate per unit of area (m/s),

q_{ini} = initial discharge or initial filtration rate per unit of area (m/s), and

b = exponent in the exponential model for filtration rate.

Table 5 presents a summary of the results obtained in each experiment, where the last two columns shows the cumulative specific filtered volume and value of the GPI index obtained at $T = 6$ hours, which corresponds to the duration of the majority of the experiments. Table 6 presents the main statistics for the GPI at this time, represented by the average, standard deviation, and coefficient of variance, CV . Additionally, the number of experiments (N) for different combinations of expanded perlite and thickness are shown

Table 3—Characteristics of each type of expanded perlite.

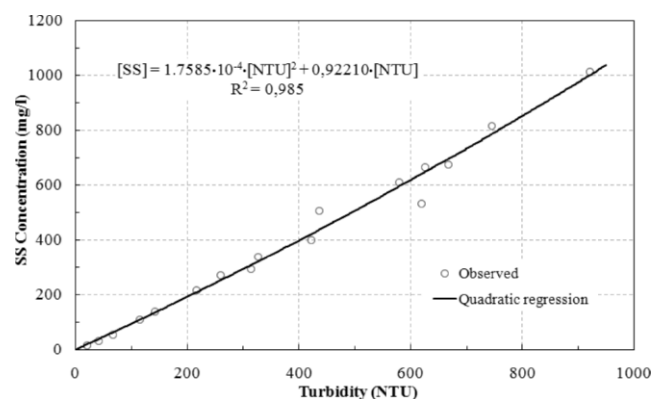
Characteristic	A-4	A-5	A-6
d_{10} (mm)	0.36	0.39	0.47
d_m (mm)	0.88	1.12	1.38
d_{60} (mm)	1.04	1.28	1.59
CU (d_{60}/d_{10})	2.90	3.26	3.37
Bulk density (kg/m^3)	170	150	130

in the last row of this table. It can be seen from Table 6 that the best two filter media are the expanded perlite A4 with either 8 or 10 cm of layer thickness, because both have the best averages and the minimum coefficients of variance. Similar results were obtained when only low input concentrations were studied ($C_{inp} < 200 \text{ mg/L}$). Finally, the largest GPI values were also observed for these two filter media in all the cases where T was less than 6 hours.

In general, the results are consistent with what was expected, considering the physical processes involved in filtration. It was anticipated that a larger thickness for the filter media would imply a reduction in filtration rate per unit of area, q , and an increase in R_T . Likely explanations for cases where this behavior did not occur were the possible existence of preferential fluxes and the clogging of fine layers of expanded perlite, which would reduce the hydraulic capacity quickly. It was also expected that the type of expanded perlite would influence the results, because larger grains imply more flux tubes, which means reductions in R_T . This behavior took place, as was expected. Regarding the effects of the hydraulic head, H , in q and R_T , an increase in q and a reduction in R_T were observed as H changed from 35 to 80 cm. If all the experiments are grouped according to the hydraulic head, average values of $q = 1321.6 \text{ L/h/m}^2$ and $R_T = 73.3\%$ are obtained when $H = 35 \text{ cm}$, while values of 3506.7 L/h/m^2 and 53.9% are observed in the experiments where $H = 80 \text{ cm}$. The classic explanation for this is given by the linear relationship between the flow velocity and the hydraulic gradient. A larger gradient produces a larger velocity and a shorter time of residence of the sediments in the filter, which means a reduction in the efficiency removal. However, it has been shown that, in other filter media, this relationship breaks down as fine sediment accumulates on the top of the surface, so the flowrate quickly becomes insensitive to H and is mainly a function of the sediments being accumulated on the filter's surface (Urbonas, 1999). This was not observed in these laboratory tests, with durations up to 33 hours, which may be too short to notice this effect. However, the different filtration media here used might also explain this observation, because, in the case of perlite, most of the sediments are retained, not on the surface, but inside the filter (Dickenson, 1992), as will be discussed later in this paper. Long-term field tests of this filter media are required to clarify this discrepancy, which is not minor, because the designer should have a good understanding of the performance of the filter media through the entire time of operation of the filter.

Table 4—Main characteristics of the geotextile.

Characteristic	Value
Mass/unit area (g/m^2)	150
Porosity O_{90} (μm)	170
Thickness (mm)	2.5
Permissivity (second^{-1})	2.0

**Figure 5—Relationship between turbidity and suspended solids (SS) concentration.**

Finally, the effects of changing the average input concentration (C_{inp}) in q and R_T were also evaluated. Because C_{inp} is not perfectly constant through each experiment, an average input concentration was computed for each of the experiments and used in this analysis. This concentration is computed as follows:

$$\bar{C}_{inp} = \frac{Lm}{\nabla \cdot R_T} \quad (5)$$

Where

Lm = cumulative removed mass during the experiment (g/m^2).

As expected, larger input concentrations reduce q . However, there were also reductions in R_T , which was not expected, because the reduction of voids in the filter media resulting from the larger number of suspended solids would not allow the solids to pass. This result is not supported by the majority of the literature devoted to the study of filter media (see CONTECH Stormwater Solutions Inc. [2002b] for a good summary), which indicates a direct relationship between influent concentration and total suspended solids (TSS) removal efficiency, defined as the relationship between influent and effluent TSS event-mean concentrations. One exemption to this corresponds to the studies by CONTECH Stormwater Solutions Inc. (2002a and 2002b), which concluded that, for perlite stormwater filters, the TSS removal efficiency can be said to quickly become constant and independent of influent TSS concentrations. However, these last two

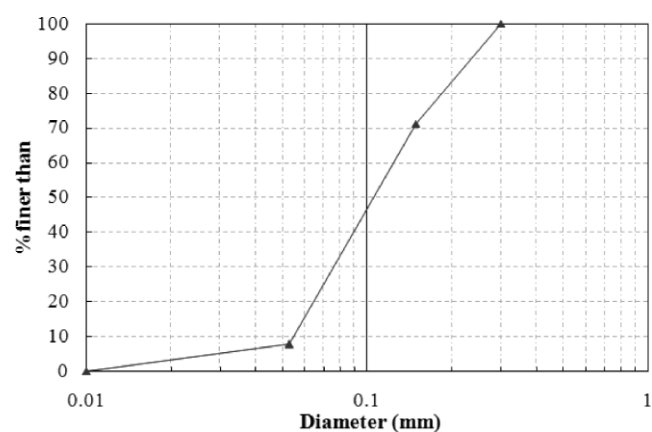
**Figure 6—Particle-size distribution of the suspended solids.**

Table 5—Summary of main results.

Experiment number		<i>T</i> (hours)	Type	<i>H</i> (cm)	<i>h</i> (cm)	<i>C</i> _{inp} (mg/L)	<i>C</i> _{out} (mg/L)	<i>Lm</i> (g/m ²)	<i>R</i> _T %	<i>q</i> _{ini} (L/s/m ²)	<i>q</i> _{end} (L/s/m ²)	<i>V</i> (<i>T</i> = 6 hours) (L/m ²)	GPI (<i>T</i> = 6 hours)
1	a	5.55	A4	35	6	65–221	15–64	1016	74.94	0.627	0.487	11419	24.45
1	b	5.55	A4	35	8	65–221	5–32	1045	89.42	0.577	0.382	9788	25.01
1	c	5.35	A4	35	10	65–221	7–25	1087	88.14	0.587	0.400	10531	26.52
2	a	6.05	A6	35	6	51–237	19–142	987	54.75	0.538	0.397	9931	15.53
2	b	6.05	A6	35	8	51–237	15–87	1057	67.48	0.492	0.357	8976	17.31
2	c	6.00	A6	35	10	51–237	13–135	1194	65.07	0.546	0.392	10682	19.86
3	a	6.15	A5	35	6	83–162	14–57	779	75.78	0.502	0.371	9167	19.85
3	b	6.10	A5	35	8	83–162	12–42	938	80.03	0.513	0.452	10568	24.16
3	c	6.10	A5	35	10	83–162	8–41	775	85.74	0.446	0.329	8034	19.68
4	a	6.05	A4	35	6	242–440	53–188	1761	68.23	0.562	0.275	8085	15.76
4	b	6.00	A4	35	8	242–440	41–146	2246	72.82	0.587	0.364	9770	20.33
4	c	6.05	A4	35	10	242–440	15–54	2001	90.69	0.474	0.216	6977	18.08
5	a	6.00	A5	35	6	252–429	84–221	1889	55.68	0.542	0.435	10186	16.20
5	b	6.10	A5	35	8	252–429	60–162	2121	67.85	0.485	0.320	9320	18.07
5	c	6.05	A5	35	10	252–429	55–179	2050	72.34	0.474	0.332	8569	17.71
6	a	5.15	A4	35	6	743–1047	313–580	3233	53.37	0.559	0.254	6904	10.53
6	b	5.15	A4	35	8	743–1047	196–472	4056	64.76	0.566	0.241	7111	13.16
6	c	5.15	A4	35	10	743–1047	37–303	3865	87.55	0.490	0.139	4758	11.90
7	a	5.15	A6	35	6	651–1047	201–713	2552	31.17	0.576	0.456	10863	9.67
7	b	5.20	A6	35	8	651–1047	187–767	2981	38.38	0.555	0.427	10314	11.31
7	c	5.20	A6	35	10	651–1047	211–639	3756	47.05	0.601	0.409	10263	13.80
8	a	4.55	A5	35	6	572–1227	365–838	2287	40.14	0.492	0.281	7360	8.44
8	b	4.55	A5	35	8	572–1227	191–494	2916	58.45	0.492	0.209	6647	11.10
8	c	4.55	A5	35	10	572–1227	162–440	3581	68.47	0.455	0.251	6514	12.74
9	a	6.00	A4	80	6	65–262	32–146	1828	52.53	1.273	0.990	24446	16.05
9	b	6.05	A4	80	8	65–262	19–130	2128	64	1.190	0.765	22154	17.72
9	c	6.00	A4	80	10	65–262	21–108	2275	66.55	1.113	0.947	23428	19.49
10	a	6.00	A5	80	6	75–216	40–142	1379	41.25	1.248	1.107	25117	12.95
10	b	6.00	A5	80	8	75–216	28–123	1632	51.18	1.213	1.026	23899	15.29
10	c	6.00	A5	80	10	75–216	20–108	1713	57.64	1.098	0.940	21645	15.60
11	a	6.05	A4	80	6	242–549	113–397	3419	45.06	1.203	0.596	21849	12.31
11	b	6.05	A4	80	8	242–549	80–334	3803	53.35	1.248	0.599	20626	13.75
11	c	6.00	A4	80	10	242–549	78–318	4343	61.07	1.379	0.705	20466	15.62
12	a	6.00	A5	80	6	242–440	104–334	2692	31.01	1.236	1.022	25337	9.82
12	b	6.00	A5	80	8	242–440	76–252	2672	52.76	1.142	0.431	15279	10.08
12	c	6.00	A5	80	10	242–440	47–365	3612	51.12	1.074	0.821	20626	13.18
13	a	31.65	A4	35	8	78–113	2–28	2472	87.31	0.516	0.104	9308	23.22
13	b	31.65	A4	35	10	78–113	3–18	3432	91.36	0.513	0.268	10150	26.49
14	a	33.00	A5	35	8	80–108	3–33	2383	72.90	0.563	0.116	10546	21.97
14	b	33.00	A5	35	10	80–108	6–31	3302	75.23	0.549	0.221	10667	22.93
15	a	18.00	A4	35	8	461–549	56–182	6020	70.72	0.506	0.081	8828	17.84
15	b	18.00	A4	35	10	461–549	87–208	7370	71.51	0.513	0.184	9388	19.18
16	a	18.00	A5	35	8	461–617	39–344	4981	59.08	0.566	0.047	9132	15.42
16	b	18.00	A5	35	10	461–617	137–318	6844	58.73	0.559	0.252	9798	16.44
17	a	32.00	A5	80	8	84–104	4–33	3493	68.52	1.043	0.053	18550	15.89
17	b	32.00	A5	80	10	84–104	28–54	5700	55.87	1.103	0.782	22731	15.88

Table 6—Main statistics of GPI (*T* = 6 hours) for different combinations of expanded perlite and thickness. A4, A5, and A6 are the types of expanded perlite, and the number after the hyphen is the thickness of the filter media (cm).

	A5-10	A5-8	A5-6	A4-10	A4-8	A4-6	A6-10	A6-8	A6-6
Mean	16.77	16.50	13.45	19.61	18.72	15.82	16.83	14.31	12.60
Standard deviation	3.35	4.85	4.66	5.37	4.47	5.36	4.29	4.24	4.14
CV	0.20	0.29	0.35	0.27	0.24	0.34	0.25	0.30	0.33
<i>N</i>	8	8	5	7	7	5	2	2	2

Table 7—Values of coefficients ki and c .

Type	H (cm)	h (cm)	ki	c
A4	35	6	0.0011	0.1416
A4	35	8	0.0011	0.1500
A4	35	10	0.0012	0.1795
A4	80	6	0.0020	0.0915
A4	80	8	0.0024	0.1247
A4	80	10	0.0016	0.0646
A5	35	6	0.0006	0.0402
A5	35	8	0.0010	0.1440
A5	35	10	0.0006	0.0758
A5	80	6	0.0013	0.0116
A5	80	8	0.0025	0.1532
A5	80	10	0.0014	0.0472
A6	35	6	0.0005	0.0094
A6	35	8	0.0005	0.0094
A6	35	10	0.0006	0.0321

studies do not explain the reduction in R_T observed in the experiments. It is possible that most of the concentrations used in the experiments were too high, and particles just passed through the filter, which would not contradict the studies with concentrations up to 350 mg/L by CONTECH Stormwater Solutions Inc. (2002a and 2002b); or there may have been particles already captured by the filter that were later released and measured in the output concentration.

Modeling the Performance of the Filtration Mixed Media

Building a model to explain the filtration process is very complex. There are various mechanisms to be considered, depend-

ing on how the removal of the particle occurs. Some of the authors reporting one or more of these processes are Bai and Tien (1997), Neufeld (1996), and Purchas (1997). In the case of stormwater filtration, the three important mechanisms are as follows:

- (1) Surface screening, in which the particle with diameter d is captured at the surface by a flux tube whose diameter is less than d ;
- (2) Deep screening, which is a similar removal process, but occurs inside the filter itself; and
- (3) Deep retention, in which the particle is captured inside a tube because of surface forces, such as the Van der Waals force.

A fourth mechanism, known as *cake filtration*, may be substantial, but it was not observed in this work.

Two global models, which do not attempt to differentiate and explain each mechanism, but rather explain the complete filtration process as a single process, were developed. The first model is dimensional and is able to reproduce the filtration process under diverse conditions. It allows estimation of the removal efficiency and filtration rate based on dimensionless variables describing the processes. The second model is a regression model, which has to be calibrated for different conditions. Additionally, a model proposed by Urbonas (1999), referred to here as the *empirical model*, is also presented and used to evaluate and compare the performance of the other two models.

Empirical Model. This model proposed by Urbonas (1999) describes the filtration rate as a function of the cumulative mass removed by the filter. It was developed to represent filtration in sand

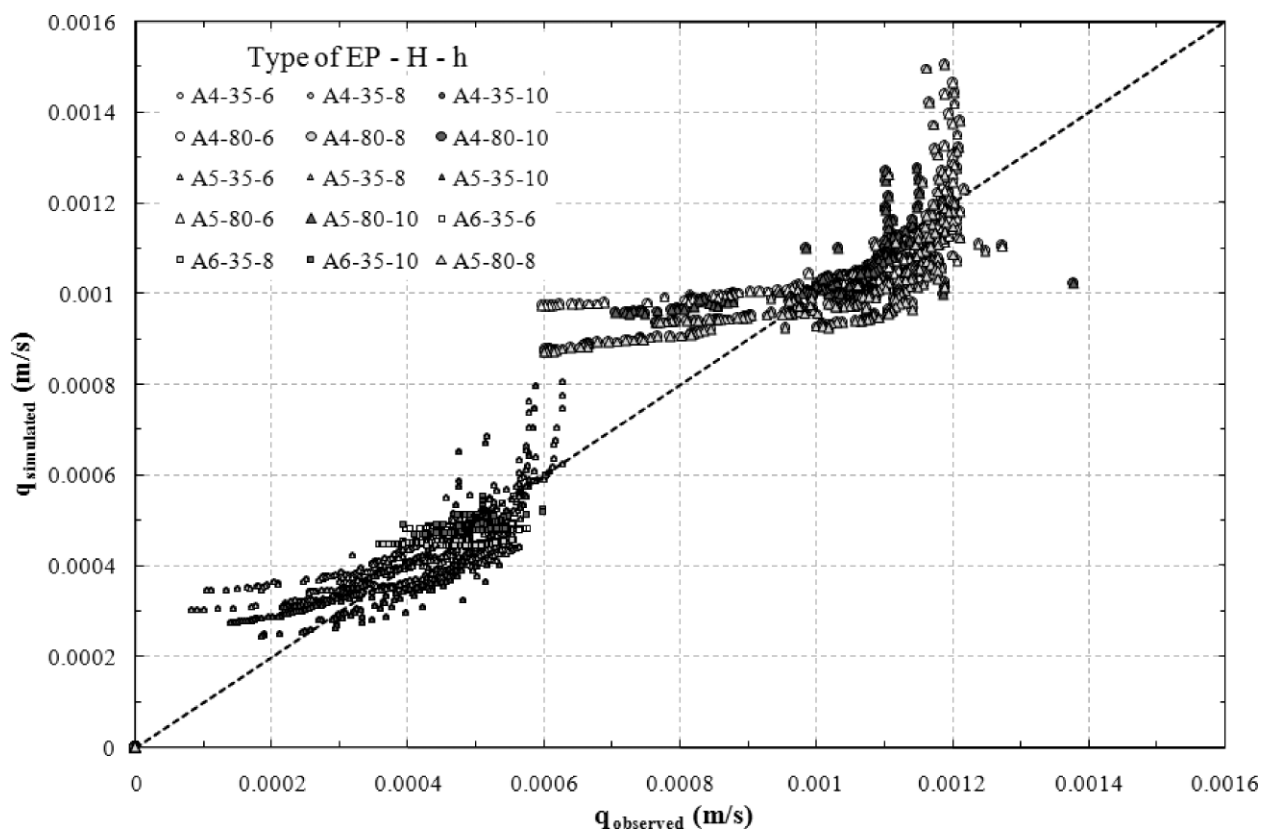
**Figure 7—Global performance of the empirical model, prediction of q .**

Table 8—Variables describing the filtration process.

Variable	Definition	Units	Type
q	Filtration rate per unit of area	m/s	Dependent
C_{inp}	Input concentration	g/m ³	Independent
C_{out}	Output concentration	g/m ³	Dependent
H	Head	m	Independent
h	Thickness of filter layer	m	Independent
d_m	Mean diameter of grains of filter media	m	Independent
CU	$CU = d_{60}/d_{10}$	—	Independent
μ	Dynamic viscosity = water viscosity	g/m · s	Independent
θ_0	Effective porosity of the filter media	—	Independent
θ_R	Ratio of cumulative volume of solids removed to filter volume	—	Dependent
ρ_s	Mass density of suspended solids = 2650 kg/m ³	g/m ³	Independent
S	Specific surface of filter media	m ⁻¹	Independent

at a time, T , and assumes that the removal efficiency, R_T , is constant and equal to 95%. The model has two parameters to be calibrated and is given by the following:

$$q = ki \cdot Lm^{-c} \tag{6}$$

$$Lm = \int_0^T (C_{inp} - C_{out}) \cdot q \cdot dt \tag{7}$$

Where

C_{out} = output concentration (g/m³), given by $(1 - R_T) \cdot C_{inp}$;
 t = time (seconds); and

ki and c = parameters to be calibrated.

An adaptation of this model was used to estimate the filtration flowrate through time. In this adaptation, observed values of C_{out} were used to compute eq 7, instead of the approximation $C_{out} = (1 - 0.95) \cdot C_{inp}$. Values of ki and c were calibrated for each group of experiments with identical conditions (same type of expanded perlite, hydraulic head, and thickness) using the laboratory results. Table 7 presents the values of these parameters. They differ for each set of conditions of operation, and it is observed that, for the same type of perlite and thickness, there is proportionality between H and ki , so that values of ki when $H = 80$ cm are approximately twice as large as those obtained when $H = 35$ cm. On the other hand, values of the exponent c decrease in 5 out of the 6 comparable cases when H increases. This reduction of c is explained by the stronger decay in the filtration rate observed in the samples working with less hydraulic head. Finally, it was detected that calibration of ki and c may minimize the effects of the removal efficiency in the performance of the model. For example, the approximation $C_{out} = (1 - 0.95) \cdot C_{inp}$ did not significantly affect the final results of the model. This last observation is also explained, in part, by high efficiencies close to 95%, for a significant portion of the experiments.

Figure 7 summarizes the performance of the model by comparing the observed and simulated filtration rates. Two clusters are observed and differentiated by the size of the plotting markers. The first cluster in the bottom left corner corresponds to all points obtained using $H = 35$ cm, while the second cluster groups all the points for which $H = 80$ cm. This illustrates the sensitivity of the filter media performance to the hydraulic head, at least for the lengths of time analyzed in this study. There is a clear tendency of this model to overestimate the filtration rates at the beginning and end of the experiments, which means that the model is not accurately representing the filtration decay as the solids are removed by the filter. This observation is probably explained by the different removal mechanisms observed in sand and perlite; while the flowrate for a sand filter quickly becomes a function of the sediment

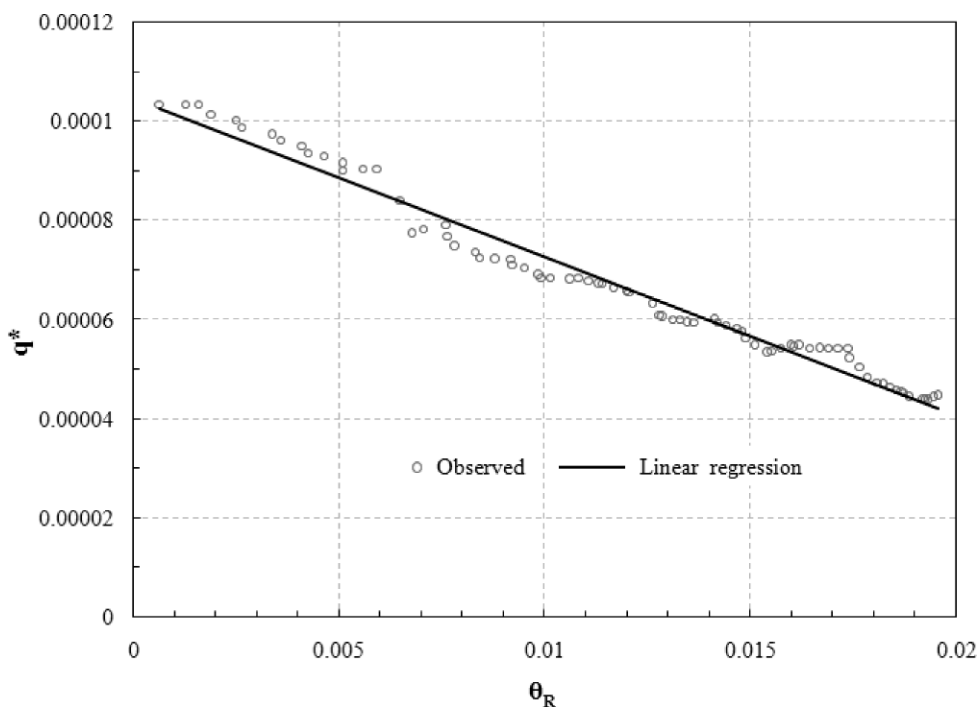


Figure 8— q^* versus θ_R for expanded perlite type A4, 800 to 1000 mg/L, and $h = 8$ cm.

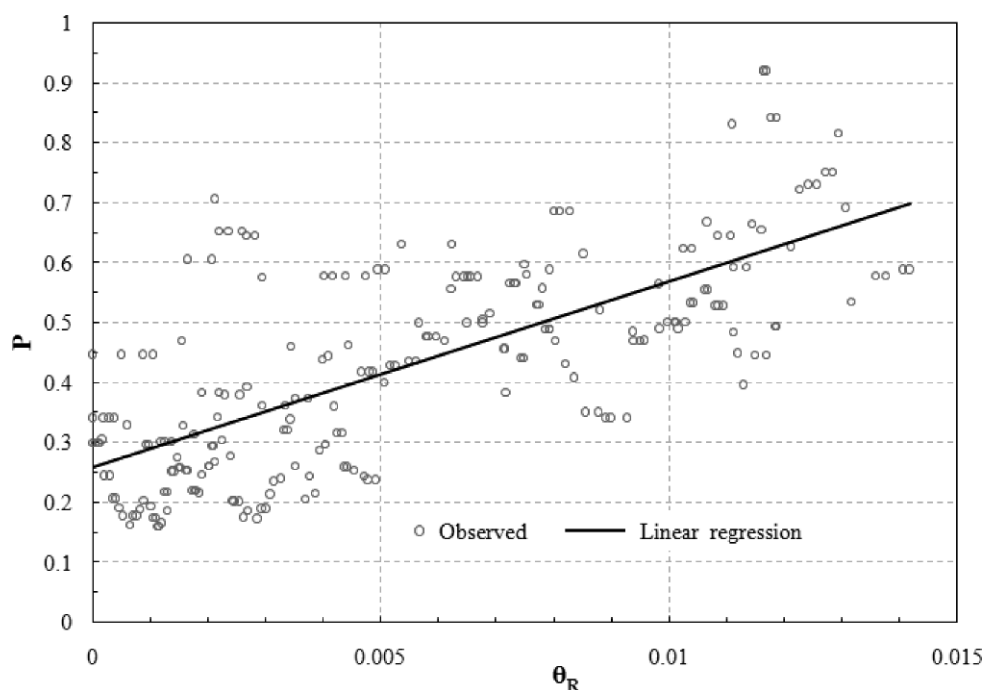


Figure 9— P versus θ_R for expanded perlite type A5, $H = 35$ cm, and $h = 6$ cm.

being accumulated on the filter surface (Urbonas, 1999), deep filtration, which does not cause this accumulation, is the main mechanism in perlite. (Dickenson, 1992). This issue will be discussed in more detail in the Conclusions section.

Dimensional Model. A dimensional analysis was performed to determine a relationship among dimensionless parameters to describe all the experiments grouped by similar geometric and hydraulic conditions. Table 8 shows the variables used in this analysis.

The analysis considers two dimensionless variables to be explained.

$$P = \frac{C_{out}}{C_{inp}} \quad (8)$$

$$q^* = \frac{q}{\sqrt{2gH}} \cdot \sqrt{\frac{h}{H}} = \sqrt{\frac{h}{2g}} \cdot \frac{q}{H} \quad (9)$$

Where

g = gravitational acceleration (m/s^2).

The variable P is the instantaneous proportion of suspended solids passing the filter, so $R = 1 - P$, and q^* is a dimensionless representation of q , proposed because, in the laboratory tests, q and H were observed to be linearly proportional.

The main assumption in developing this model is that both q^* and P are related to θ_R , which corresponds to the ratio between the

volume of retained solids by the filter during a time, $t = T$, and the total volume of the filter, and can be computed as follows:

$$\theta_R = \int_0^T \frac{(C_{inp} - C_{out}) \cdot q \cdot dt}{\rho_s \cdot h} \quad (10)$$

Where

ρ_s = mass density (g/m^3), and
 h = thickness of filter layer (m).

Because the volume of voids in the filter media is the only space where the removed solids can go, the volume of retained solids by the filter during a time $t = T$ corresponds to the reduction of the volume of voids at that time. Therefore, θ_R is equivalent to the reduction of the porosity at time $t = T$, as a result of the retention of suspended solids in the filter.

Thus, q^* and P can be expressed as functions of θ_R ; a fixed reference concentration, C_{ref} , and the other independent variables, as follows:

$$q^* = \sqrt{\frac{h}{2g}} \cdot \frac{q}{H} = f_1 \left(h, d_m, CU, \theta_0, \theta_R, S, \frac{C_{inp}}{C_{ref}} \right) \quad (11)$$

$$P = \frac{C_{out}}{C_{inp}} = f_2(h, H, d_m, CU, \theta_0, \theta_R, S) \quad (12)$$

Where

Table 9—Reference values for parameters of the dimensional model.

Parameter	u	v	m	n
Value	0.003 to 0.004	9.5×10^{-5} to 10.5×10^{-5}	10 to 14	0.30 to 0.35

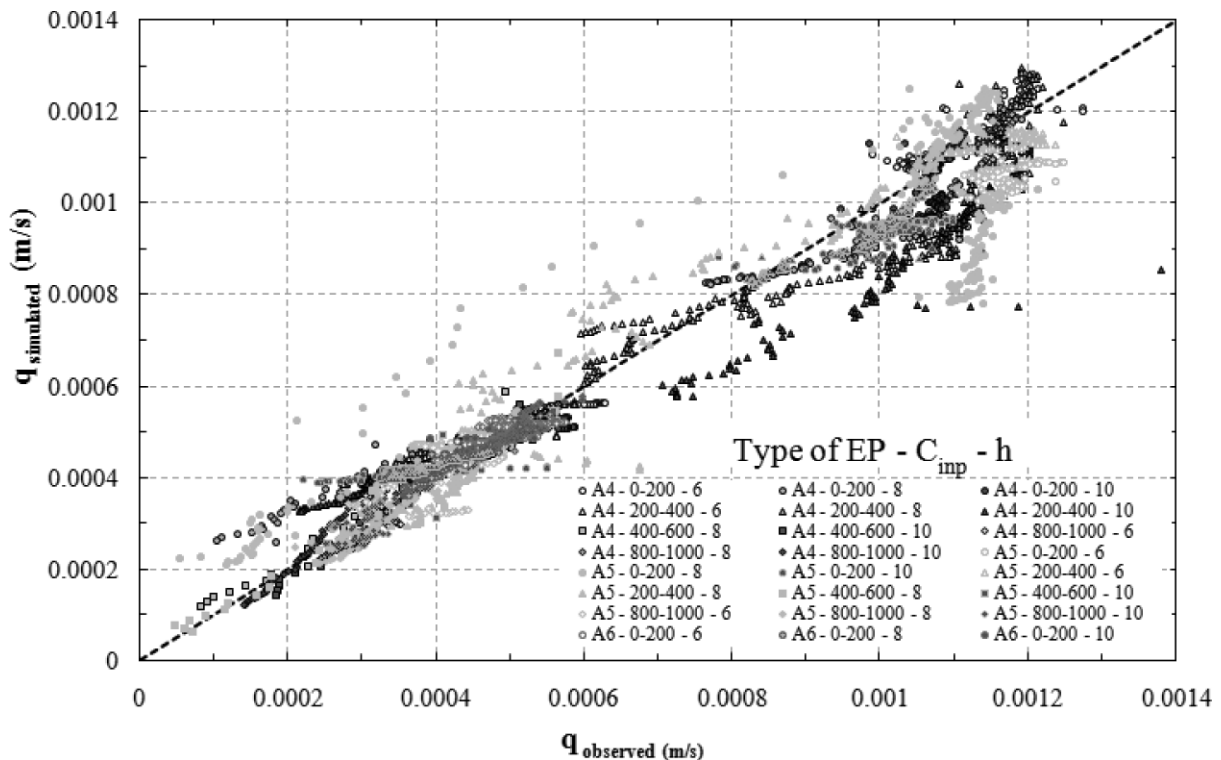


Figure 10—Global performance of the dimensional model, prediction of q .

- d_m = mean diameter of grains of filter media (m),
- CU = coefficient of uniformity,
- θ_0 = effective porosity of the filter media,
- S = specific surface area (m^{-1}), and
- C_{ref} = reference concentration (g/m^3).

In eq 11, the expression for q^* has $n_1 = 3$ dimensional variables, involves $r_1 = 1$ dimension, and there are 4 dimensionless variables. Therefore q^* can be rewritten as function of $n_1 - r_1 + 4 = 6$ dimensionless variables. In eq 12, the expression for P has $n_2 = 4$ dimensional variables, involves $r_2 = 1$ dimension, and there are 3 dimensionless variables. Then, P can be rewritten as function of $n_2 - r_2 + 3 = 6$ dimensionless variables. The new expressions are as follows:

$$q^* = \sqrt{\frac{h}{2g}} \cdot \frac{q}{H} = g_1 \left(\frac{h}{d_m}, CU, \theta_0, \theta_R, h \cdot S, \frac{C_{inp}}{C_{ref}} \right) \quad (13)$$

$$P = \frac{C_{out}}{C_{inp}} = g_2 \left(\frac{h}{H}, \frac{h}{d_m}, CU, \theta_0, \theta_R, h \cdot S \right) \quad (14)$$

From the laboratory results and as seen in Figure 8, representing one of the groups of experiences with similar geometric and hydraulic conditions, a linear relationship between q^* and θ_R was observed, given by $q^* = -u \cdot \theta_R + v$. Parameters u and v change for different experiments, which were grouped according to the type of expanded perlite, range of concentration used, and thickness of the expanded perlite layer.

A similar analysis can be done to study the variable P , which also leads to linear relationships representing each group of experiences given by $P = m \cdot \theta_R + n$, as seen in Figure 9. In this case, experiments were grouped by type of expanded perlite, thickness

of the expanded perlite layer, and head. The linear trend was not always clear, but it was assumed as a first approximation to represent the relationship between these variables. Considering all the results obtained for q^* and P , it is possible to set typical values that are suggested for a predesign step and presented in Table 9.

These two linear relationships and eq 10 can be solved for each time, t_n , using finite differences for $\theta_R^{t_n}$, q^{t_n} , and $C_{out}^{t_n}$.

The results of the dimensional model are summarized in Figures 10 and 11. Figure 10 shows the performance of the model predicting q , while Figure 11 shows the performance in predicting C_{out} . The model is able to predict the filtration rates pretty well, but the accuracy reduces as filtration rates increase. On the other hand, more scattering is observed in the prediction of C_{out} for a larger concentration, and there is a slight tendency to underestimate these concentrations as C_{inp} increases.

Regression Model. Several statistics tests were performed to build a statistical or stochastic model between the time series m_{inp} and m_{out} , which are the input and output mass per unit of area through the filter for a time Δt , respectively. These variables are computed as follows:

$$m_{inp} = \int_{t_1}^{t_2} C_{inp} \cdot q \cdot dt \approx \left(\frac{C_{inp}^{t_1} + C_{inp}^{t_2}}{2} \right) \cdot \left(\frac{q^{t_1} + q^{t_2}}{2} \right) \cdot (t_2 - t_1) \quad (15)$$

$$m_{out} = \int_{t_1}^{t_2} C_{out} \cdot q \cdot dt \approx \left(\frac{C_{out}^{t_1} + C_{out}^{t_2}}{2} \right) \cdot \left(\frac{q^{t_1} + q^{t_2}}{2} \right) \cdot (t_2 - t_1) \quad (16)$$

Where

- m_{inp} = input mass per unit of area through the filter for a time Δt , and
- m_{out} = output mass per unit of area through the filter for a time Δt .

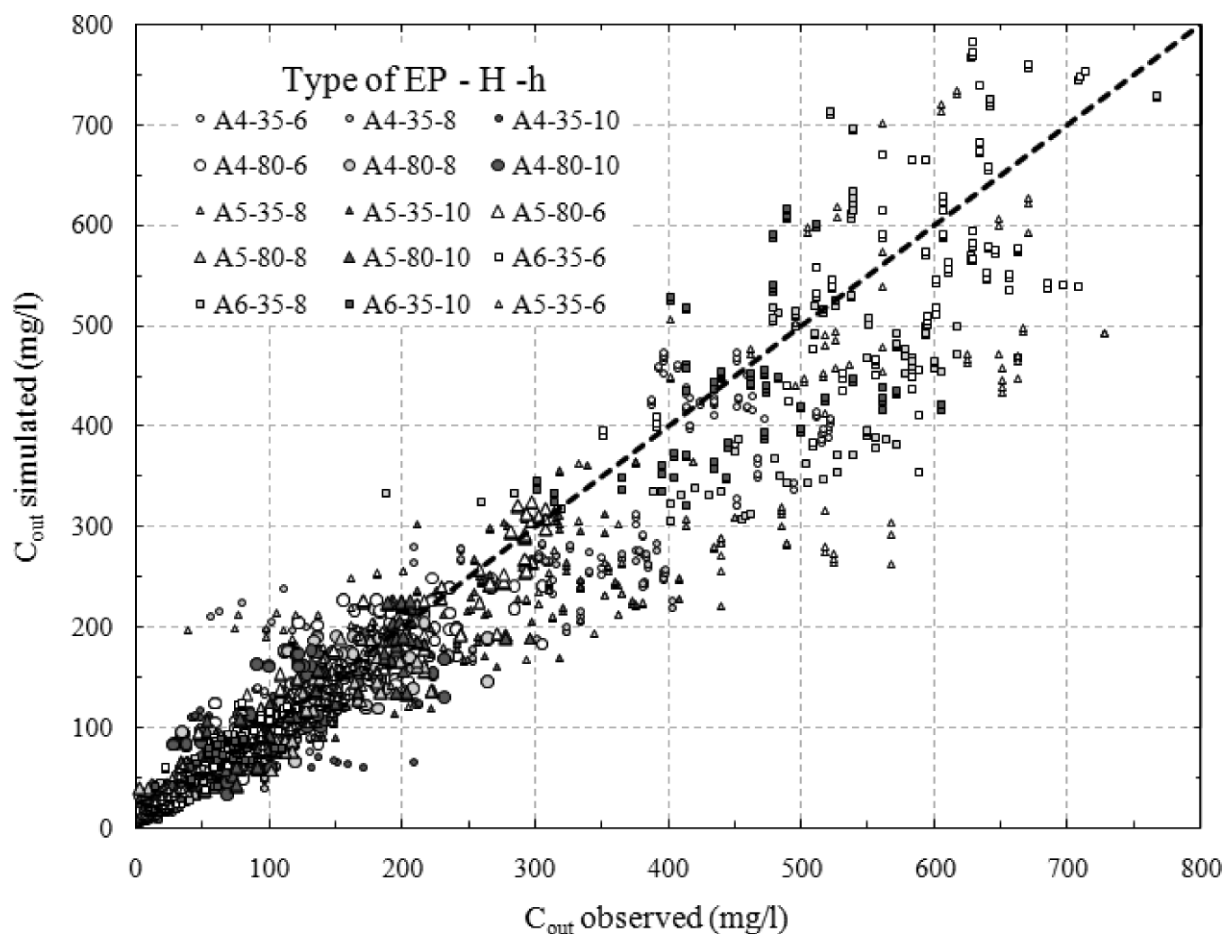


Figure 11—Global performance of the dimensional model, prediction of C_{out} .

Using simple correlation analysis, the simple autocorrelation function, and the cross-correlation function, it was determined that there is a linear dependence between both series, which are not autocorrelated. Hence, a linear regression model between m_{inp} and m_{out} , given by $m_{out} = P \cdot m_{inp}$, is assumed. The variable P is the fraction of suspended solids passing the filter without being removed.

It was decided to define P as a function of the independent variables characterizing both the filter media and the different conditions of operation, as defined in Table 8. Several linear and higher order regressions and other nonlinear relationships were tested to define P and the variables to which it is related. It was found that a multiple linear regression of the independent variables H , h , and d_m reasonably explains the observed values of P . Regression of higher order did not significantly improve the representation of this parameter. Equation 17 shows the final expression for P , whose coefficients p_1 , p_2 , p_3 , and p_4 were calibrated to reproduce the observed values of P at each experiment. Finally, C_{out} is computed using eq 18.

$$P = f(H, h, d_m) = p_1 + p_2 \cdot H + p_3 \cdot h + p_4 \cdot d_m \quad (17)$$

$$C_{out}^{t+1} = (p_1 + p_2 \cdot H + p_3 \cdot h + p_4 \cdot d_m) \cdot (C_{inp}^t + C_{inp}^{t+1}) - C_{out}^t \quad (18)$$

Where

p_i ($i = 1:4$) = coefficients for linear regression defining P .

The variation of q through time can also be modeled. However, there is not a time series for a variable that may explain this

variation, and there is dependency between q and the removed mass, as proposed by Urbonas (1999).

The decays observed for q lead to the use of an exponential decay model, with parameters a and b to reproduce the behavior of the variable through time (see eq 3). After testing several linear and higher order regressions and other nonlinear relationships, it was observed that a and b can be expressed as linear functions of H , h , and d_m —the same independent variables used in the computation of C_{out} . More mathematically complex relationships did not greatly enhance the estimation of these parameters. Additionally, it was determined that \bar{C}_{inp} (given by eq 5) also contributed to the previous variables in explaining a and b , and this contribution was also considered to be linear. Equations 19 and 20 present the final regressions to compute the parameters of the exponential model, while eq 21 shows the final model to compute q .

$$\begin{aligned} a &= f(H, h, d_m, \bar{C}_{inp}) \\ &= A_0 + A_1 \cdot H + A_2 \cdot h + A_3 \cdot d_m + A_4 \cdot \bar{C}_{inp} \end{aligned} \quad (19)$$

$$\begin{aligned} b &= f(H, h, d_m, \bar{C}_{inp}) \\ &= B_0 + B_1 \cdot H + B_2 \cdot h + B_3 \cdot d_m + B_4 \cdot \bar{C}_{inp} \end{aligned} \quad (20)$$

$$\begin{aligned} q(t) &= a \cdot e^{-b \cdot t} \\ &= (A_0 + A_1 \cdot H + A_2 \cdot h + A_3 \cdot d_m + A_4 \cdot \bar{C}_{inp}) \cdot \\ &\quad e^{-(B_0 + B_1 \cdot H + B_2 \cdot h + B_3 \cdot d_m + B_4 \cdot \bar{C}_{inp}) \cdot t} \end{aligned} \quad (21)$$

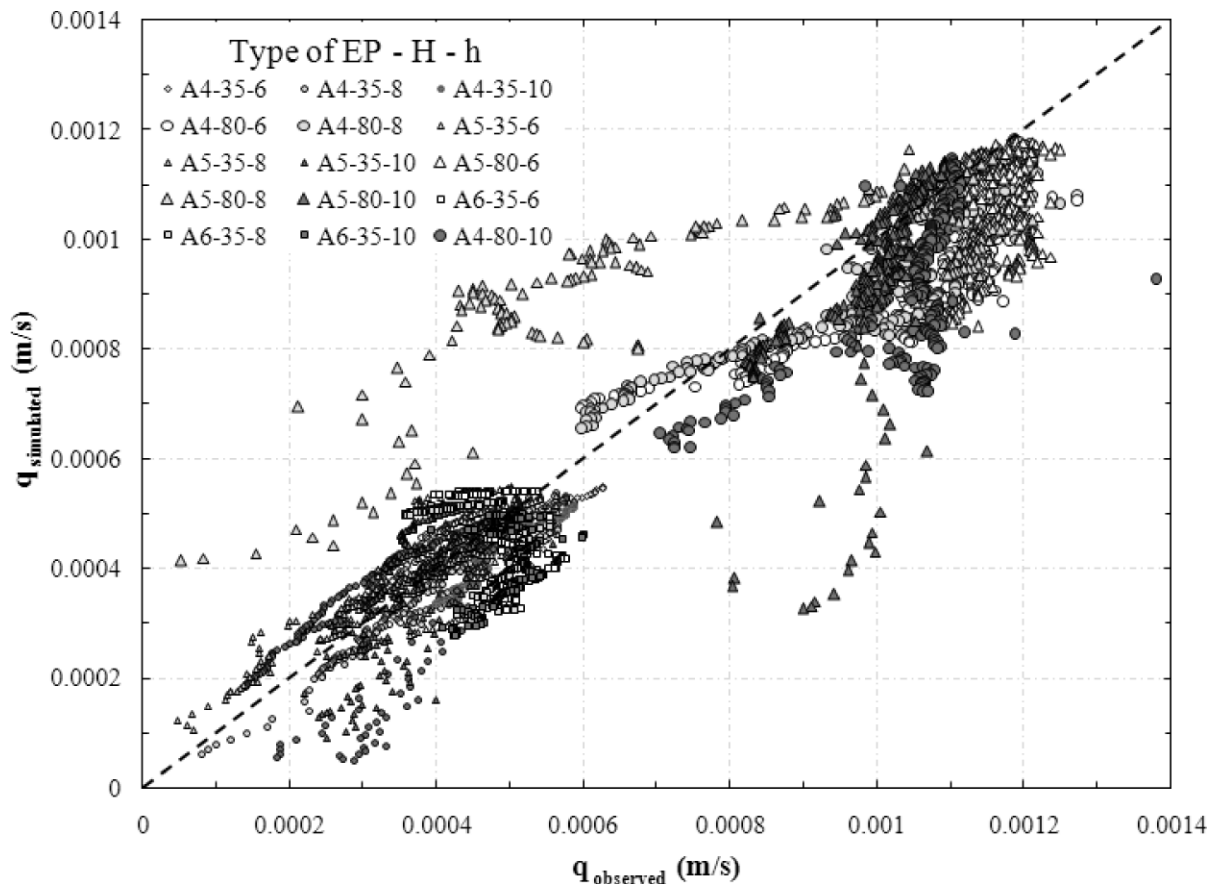


Figure 12—Global performance of the regression model, prediction of q .

Where

A_i ($i = 0:4$) = coefficients for linear regression defining a ,
 \bar{C}_{inp} = average input concentration (g/m^3), and
 B_i ($i = 0:4$) = coefficients for linear regression defining b .

The two final expressions (eqs 18 and 21) correspond to a very simple representation of the performance of the filter media and do not take into account possible interactions between the independent variables, which were assumed to be non-existent. On the other hand, no significant improvements occur when more complex relationships are defined. These two points justify the use of this model. A summary of the results of the exponential model for q and the linear regression model for C_{out} are presented in Figures 12 and 13. Again, it is possible to observe two clusters differentiated by H , as was pointed out in the Empirical Model section. On the other hand, Figure 13 shows a tendency of the regression model to underestimate C_{out} for larger concentrations. This tendency is stronger than the one observed in the dimensional model.

Conclusions

Expanded perlite, while supported by a downstream geotextile layer, is an attractive option to be used as a filter media in standardized filters designed to remove suspended solids from stormwater because of its convenient physical characteristics, neutral chemical composition, and good performance in removing the typical suspended solids found in stormwater.

For the range of thickness of expanded perlite layers used in this investigation, laboratory experiments showed that this geometric parameter does not affect the filtration rate substantially, as was expected, but greatly affects the removal efficiency (R), because a strong proportionality between thickness and R was found. This shows that the thickness of a filter is a relevant factor in suspended solids removal, in cases where porous media with high-tortuosity flow paths, such as expanded perlite, are used. As the thickness increases, it is less probable that solid particles will pass the filter without making contact with the filter grain (Gronow, 1986). This confirms that deep screening is the prevailing mechanism of filtration in this type of filter media. This characteristic of porous media should be taken into account in cases where models developed for other types of materials, particularly sand, are used to evaluate the filter performance. Similar caution is required when empirical models, developed from studies where depth may not be a factor affecting the removal efficiency, are planned to be used with relatively small filters of expanded perlite or other porous media in general. Results show that the 10-cm expanded perlite class A4 layer was the best combination, according to the GPI, an index developed to evaluate the filter performance, which can be used to analyze and compare diverse filter medias and pollutants concentrations.

The dimensional model developed here reproduces the filtration rates and output concentration better than a comparable empirical model and a regression model. Additionally, the theoretical background supporting this model is more complete, making the

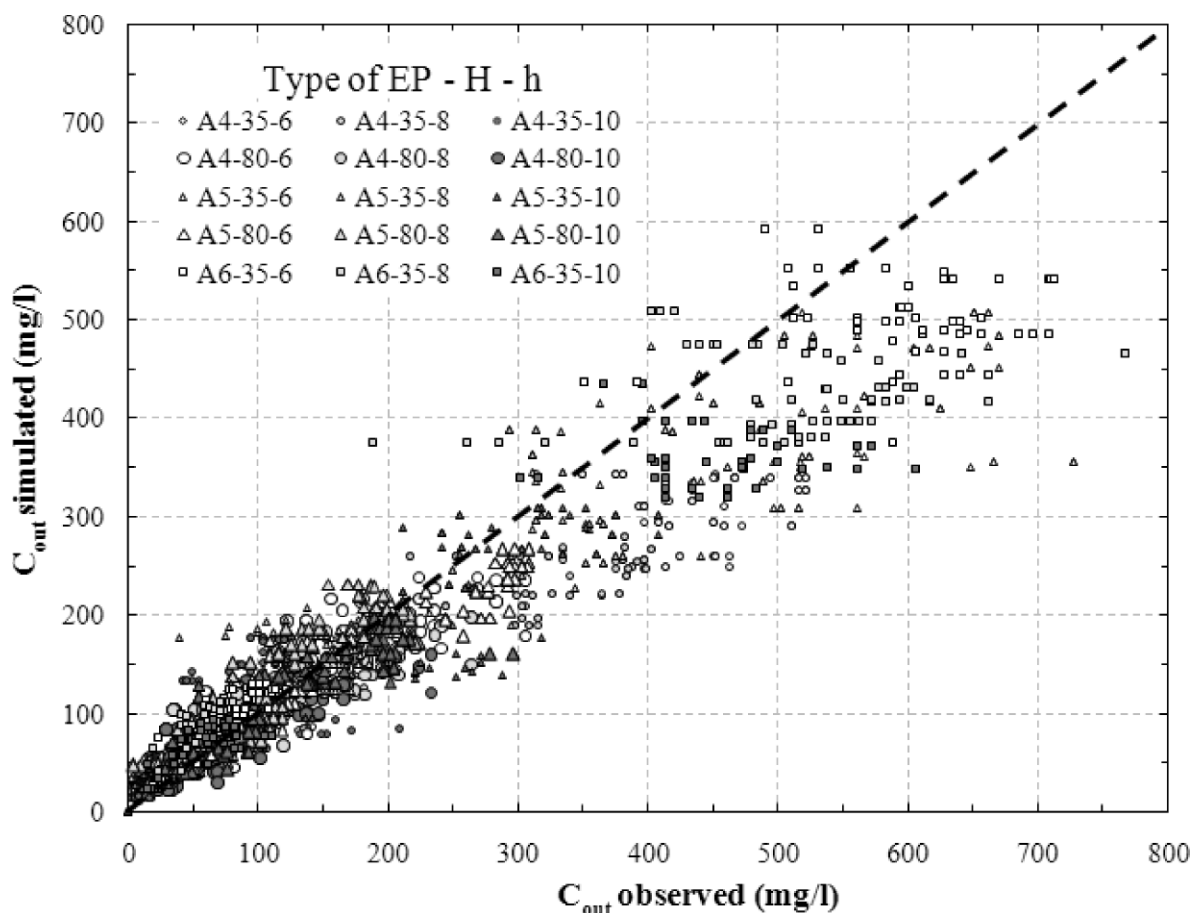


Figure 13—Global performance of the regression model, prediction of C_{out} .

dimensional model a good approach to study the filtration of suspended solids in any porous media in a filtration system not controlled by cake filtration phenomena.

A future investigation may consider the modeling and evaluation of a real expanded perlite filter by designing field tests. In real conditions, filters have intermittent operation and typically operate for much longer durations than the ones analyzed in this study, which operated for up to 33 hours. During the filter's life, not only can a wide range of very different runoff events occur, but also the internal structure of the filter media can change, which may also affect the filter performance. On the other hand, the filter media may have a longer life when there is an adequate maintenance program. Finally, these field tests would clarify the long-term dependence between the filtration rate and hydraulic gradient, because behavior was observed that is different than that previously reported in the literature for sand filters.

Credits

The authors gratefully acknowledge the financial support of CONICYT Chile through the project FONDEF D00I011 and Larry Roesner, Colorado State University (Fort Collins, Colorado) for his collaboration in this research. The comments and suggestions of the reviewers are also gratefully acknowledged.

Submitted for publication June 30, 2006; revised manuscript submitted August 24, 2007; accepted for publication December 6, 2007.

The deadline to submit Discussions of this paper is September 15, 2008.

Nomenclature

a = Coefficient in the exponential model for filtration rate.

A = Cross-sectional area of the filter (m^2).

A_i ($i = 0:4$) = Coefficients for linear regression defining a .

b = Exponent in the exponential model for filtration rate.

B_i ($i = 0:4$) = Coefficients for linear regression defining b .

c = Exponent in the empirical model for filtration rate.

C_{inp} = Input concentration (g/m^3).

\bar{C}_{inp} = Average input concentration (g/m^3).

C_{out} = Output concentration (g/m^3).

C_{ref} = Reference concentration (g/m^3).

CU = Coefficient of uniformity.

CV = Coefficient of variance.

d = Particle diameter (m).

d_m = Mean diameter of grains of filter media (m).

GPI = Global Performance Index.

h = Thickness of filter layer (m).

H = Hydraulic head (m).

ki = Coefficient in the empirical model for filtration rate.

Lm = Cumulative mass removed per unit of surface (g/m^2).

m = Parameter for the linear model between P and θ_R .

m_{inp} = Input mass per unit of area through the filter for a time Δt (g/m^2).

m_{out} = Output mass per unit of area through the filter for a time Δt (g/m^2).

n = Parameter for the linear model between P and θ_R .

p_i ($i = 1:4$) = Coefficients for linear regression defining P .

P = Instantaneous proportion of suspended solids passing the filter.

q = Filtration rate per unit of area (m/s).

q^* = Dimensionless filtration rate per unit of area.

Q = Discharge or filtration rate (m^3/s).

q_{end} = Final discharge or final filtration rate per unit of area.

q_{ini} = Initial discharge or initial filtration rate per unit of area.

R = Efficiency removal (%).

R_T = Total efficiency removal (%).

S = Specific surface area (m^{-1}).

T or t = Time (seconds or hours).

u = Parameter for the linear model between q^* and θ_R .

v = Parameter for the linear model between q^* and θ_R .

\forall = Cumulative specific filtered volume (m^3/m^2).

μ = Dynamic viscosity ($\text{g}/\text{m} \cdot \text{s}$).

ρ_s = Mass density (g/m^3).

θ_0 = Effective porosity of the filter media.

θ_R = Ratio of cumulative volume of solids removed to filter volume.

References

- Adriasola, J. M. (2003) Design of a Modular Filter for Stormwater Treatment (Diseño de un filtro modular para aguas lluvias). Masters thesis, Pontificia Universidad Católica de Chile, Chile (in Spanish).
- American Public Health Association; American Water Works Association; Water Environment Federation (1998) *Standard Methods for the Examination of Water and Wastewater*, 20th ed.; American Public Health Association: Washington, D.C.
- ASTM (1997) Standard Test Method for Sieve Analysis of Fine and Coarse Aggregates, C 136-96a. *Annual Book of ASTM Standards*; American Society for Testing and Materials: West Conshohocken, Pennsylvania.
- Bai, R.; Tien, C. (1997) Particle Detachment in Deep-Bed Filtration. *J. Colloid Interface Sci.*, **186**, 307–317.
- CALTRANS (2004) BMP Retrofit Pilot Program, Final Report, Report ID CTSW-RT-01-050; California Department of Transportation, Division of Environmental Analysis: Sacramento, California.
- Clark, S.; Pitt, R. (1999) *Stormwater Treatment at Critical Areas, Evaluation of Filtration Media*, EPA-600/R-00/010; U.S. Environmental Protection Agency, Water Supply and Water Resources Division, National Risk Management Laboratory: Cincinnati, Ohio.
- CONTECH Stormwater Solutions Inc. (2002a) Sandy Loam TSS Removal Efficiency of a Stormwater BMP: Coarse Perlite Stormfilter Cartridge at 57 L/min (15 gpm), Report No. PE-B023; CONTECH Stormwater Solutions Inc.: Portland, Oregon.
- CONTECH Stormwater Solutions Inc. (2002b) Silt Loam TSS Removal Efficiency of a Stormwater BMP: Coarse/Fine Perlite Stormfilter Cartridge at 28 L/min (7.5 gpm), Report No. PE-B013; CONTECH Stormwater Solutions Inc.: Portland, Oregon.
- Dechesne, M.; Barraud, S.; Bardin, J. P. (2002) Performance of Stormwater Infiltration Basins on the Long Term. *Proceedings of the 9th International Conference on Urban Drainage (9ICUD)*, Sept. 8–13, Portland, Oregon; ASCE Publications: Reston, Virginia [CD-ROM].
- Demirbas, O.; Alkan, M.; Dogan, M. (2002) The Removal of Victoria Blue from Aqueous Solution by Adsorption on a Low-Cost Material. *Adsorption*, **8** (4), 341–349.
- Dickenson, C. (1992) *Filters and Filtration Handbook*, 3rd ed.; Elsevier Advanced Technology: Oxford, United Kingdom.
- Dogan, M.; Alkan, M. (2003) Removal of Methyl Violet from Aqueous Solution by Perlite. *J. Colloid Interface Sci.*, **267**, 32–41.
- Dogan, M.; Alkan, M.; Turkyilmaz, A.; Ozdemir, Y. (2004) Kinetics and Mechanism of Removal of Methylene Blue by Adsorption Onto Perlite. *J. Hazard. Mater.*, **109** (1–3), 141–148.
- Gronow, J. R. (1986) Mechanisms of Particle Movement in Porous Media *Clay Miner.*, **21** (4), 753–767.
- Hernández, M. A.; Rojas, F.; Corona, L.; Lara, V. H.; Portillo, R.; Salgado, M. A.; Petranoskii, V. (2005) Evaluation of the Porosity in Natural Zeolites Using Differential Curves of Adsorption (Evaluación de la porosidad de zeolitas naturales por medio de curvas diferenciales de adsorción). *Rev. Int. Contam. Ambient.*, **21** (2), 71–81 (in Spanish).
- Joseph, C.; Rodier, C. (1994) Renovation of Domestic Waste-Water by Unsaturated Filtration in a Bed of Expanded Perlite. *Environ. Technol.*, **15** (7), 631–643.
- Kennes, C.; Thalasso, F. (1998) Review: Waste Gas Biotreatment Technology. *J. Chem. Technol. Biotechnol.*, **72** (4), 303–319.
- Kleineidam, S.; Schüth, C.; Grathwohl, P. (2002) Solubility-Normalized Combined Adsorption-Partitioning Sorption Isotherms for Organic Pollutants. *Environ. Sci. Technol.*, **36** (21), 4689–4697.
- Milesi, C.; de Ridder, S.; DeLeon, D.; Wachter, H. (2006) A Comparison of Two Media Filtration Bmp Treatments for the Removal of PAHs and Phthalates from Roadway Runoff. *Proceedings of StormCon 2006: 5th Annual North American Surface Water Quality Conference and Exposition*, Denver, Colorado, July 24–27; ForesterPress: Santa Barbara, California.
- MOP-DICTUC (2001) Analysis of Stormwater Runoff Quality in Infiltration Wells in the City of Santiago (Análisis de la calidad de las aguas lluvias urbanas en pozos de infiltración en la ciudad de Santiago), Final report; Hydraulic Infrastructure Division, Ministry of Civil Works and DICTUC, Department of Hydraulic and Environmental Engineering, Catholic University, Santiago, Chile (in Spanish).
- Neufeld, C. Y. (1996) An Investigation of Different Media for Filtration of Stormwater. Masters Thesis, Department of Civil Engineering, University of Colorado at Denver.
- Perlite Institute Inc. (2007) Basic Facts About Perlite...The World's Most Versatile Mineral. Perlite Institute Inc.: Harrisburg, Pennsylvania, http://www.perlite.org/perlite_info/guides/general_info/basic_facts.pdf (accessed December 2007).
- Purchas, D. (1997) *Handbook of Filter Media*; Elsevier Advanced Technology: Oxford, United Kingdom.
- Raimbault, G.; Nadji, D.; Gauthier, C. (2000) Stormwater Infiltration and Porous Material Clogging. Division EAU, Central Laboratory of Bridges and Roads (Laboratoire Central des Ponts et Chaussées), Bouguenais, France.
- Ramírez-López, E.; Corona-Hernández, J.; Dendooven, L.; Rangel, P.; Thalasso, F. (2003) Characterization of Five Agricultural By-Products as Potential Biofilter Carriers. *Bioresour. Technol.*, **88** (3), 259–263.
- Rinker Material Corporation (2002) Particle Size Distribution (PSD) in Stormwater Runoff. Info Briefs. Department of Development and Research, Rinker Materials Corporation: West Palm Beach, Florida.
- Smet, E.; Chasaya, G.; Van Langenhove, H.; Verstraete, W. (1996) The Effect of Inoculation and the Type of Carrier Material Used on the Biofiltration of Methyl Sulphides. *Appl. Microbiol. Biotechnol.*, **45** (1–2), 293–298.
- Timmons, M. B.; Holder, J. L.; Ebeling, J. M. (2006) Application of Microbead Biological Filters. *Aquacult. Eng.*, **34** (3), 332–343.
- Uluatam, S. S. (1991) Assessing Perlite as a Sand Substitute in Filtration. *J. Am. Water Works Assoc.*, **83** (6), 70–71.
- Urbonas, B. (1999) Design of a Sand Filter for Stormwater Quality Enhancement. *Water Environ. Res.*, **71**, 102–111.
- Urbonas, B.; Stahre, P. (1993) *Stormwater: Best Management Practices and Detention for Water Quality, Drainage, and CSO Management*; Prentice Hall: Englewood Cliffs, New Jersey.

- U.S. Environmental Protection Agency (2005) *Stormwater Management, Inc. CatchBasin StormFilter™. Environmental Technology Verification Report, Stormwater Source Area Treatment Device*, EPA-600/R-05/138. Report prepared by Environmental Consulting & Technology Inc., Edison, New Jersey; U.S. Environmental Protection Agency: Washington, D.C.
- Wigginton, B. O.; de Ridder, S. (1999) *Sediment Loading on a Perlite Filled Stormfilter Cartridge*. Stormwater Management: Portland, Oregon.
- Zilli, M.; Fabiano, B.; Ferraiolo, A.; Converti, A. (1996) Macro-Kinetic Investigation on Phenol Uptake from Air by Biofiltration: Influence of Superficial Gas Flow Rate and Inlet Pollutant Concentration. *Biotechnol. Bioeng.*, **49** (4), 391–398.